I&EC research
Industrial & Engineering Chemistry Research

Article

Cite This: Ind. Eng. Chem. Res. 2019, 58, 21312−21322

pubs.acs.org/IECR

Synthesis of Branched Poly(butyl acrylate) Using the Strathclyde Method in Continuous-Flow Microreactors

Liang Xiang,[†] Yang Song,[†] Min Qiu,[†] and Yuanhai Su*[,†,‡]

[†]Department of Chemical Engineering, School of Chemistry and Chemical Engineering, and [‡]Key Laboratory of Thin Film and Microfabrication (Ministry of Education), Shanghai Jiao Tong University, Shanghai 200240, P. R. China

Supporting Information

ABSTRACT: Solution polymerization of butyl acrylate and divinylbenzene (DVB) in toluene, initiated with 2,2′-azobisisobutyronitrile and mediated with chain transfer agent dodecanethiol (DDT), was carried out in a capillary microreactor with a 1 mm inner diameter. Through the Strathclyde method, branched poly(butyl acrylate) with different molecular weight distributions (MWDs) was prepared by adjusting the feed formulation and the residence time. The dosages of DVB and DDT were controlled to avoid gelation, and their effects on the branching degree of the products were investigated. The multimodal MWDs were deconvoluted to quantitatively study the branching process. The kinetics in batch and continuous operation are compared. Aqueous miniemulsion polymerization with a similar feed formulation was also conducted in the microreactor, enabling faster reaction rate, lower solution viscosity, and higher branching efficiency. This study demonstrated the feasibility to use commercial monomers to prepare branched polymers with high functionality and a dense architecture in continuous-flow mode.

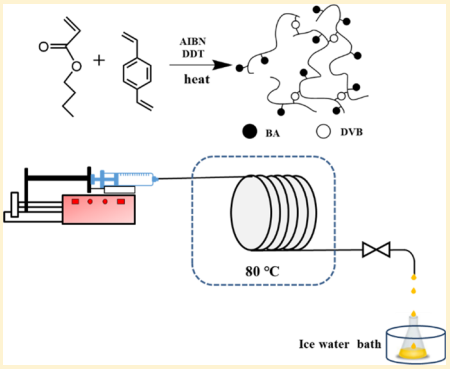

1. INTRODUCTION

Since Flory[1] proposed the concept of branched polymers in 1952, and Kim[2] synthesized hyperbranched polyphenyl in 1987, branched polymers including dendritic, highly- and hyper-branched, and multibranched systems have gradually attracted academic attention owing to their fancy architectures and versatile properties.[3,4] Branched polymers generally feature lower glass transition temperature,[5] lower melt rheology, improved solubility,[6] higher encapsulation capacity, and possess more functional end groups[7] compared to their linear counterparts of the same molecular weights. Besides, in combination with postpolymerization modification, branched polymers have various high-performance applications in flocculants, viscosity modifiers,[8] catalyst supports,[9] functional optoelectronic materials,[10] and in the biomedical field, which takes advantage of the cavities formed in densely branched structures for drug delivery.[11,12]

Polycondensation using AB_x[13] type or multifunctional A_2 and B_3[14] monomers is the most common method for synthesizing branched polymers, focusing primarily on branched polyesters and polyurethanes. However, most of these synthetic routes require the presence of certain functional groups such as alcohols and isocyanates, or specially designed catalysts.[15] Self-condensing vinyl polymerization (SCVP) proposed by Frechet[16] in 1995 has led to a significant advance in the synthesis of branched polymers. SCVP is based on the use of the inimer, that is, a vinyl monomer with an additional functional moiety capable of being activated and initiating the polymerization of other vinyl groups. SCVP has been expanded to a variety of living polymerization techniques[17−19] such as ionic polymerization, ring-opening polymerization, and controlled radical polymerization. Despite receiving much attention, one major drawback of SCVP is that most reported monomers are not commercially available and require synthesis on demand. In 2000, Sherrington et al.[5,20] suggested a novel synthesis approach commonly known as the Strathclyde method. In the presence of thiols, gel formation is suppressed by extensive chain transfer, and monovinyl monomers can be copolymerized with low levels of multivinyl monomers to prepare long-chain branched polymers, which proved to be a cost-effective route suitable for a range of vinyl monomers, including styrene,[21,22] methyl methacrylate,[5,20,23] and vinyl acetate.[24]

Continuous polymerization processes are always preferred in the industrial production of bulk polymers. In recent years, microreactor technology has attracted great attention in the preparation of special polymer products. Microreactors have faster heat and mass transfer rates because of their higher surface-to-volume ratio compared to conventional batch reactors, effectively minimizing inhomogeneity of various substance concentrations and occurrence of hot spots in highly exothermic polymerization of vinyl monomers. Moreover, microreactors can be readily scaled up to satisfy industrial

Received: July 17, 2019
Revised: October 25, 2019
Accepted: October 31, 2019
Published: October 31, 2019

DOI: 10.1021/acs.iecr.9b03906
Ind. Eng. Chem. Res. 2019, 58, 21312−21322

production through operating multiple tubes in parallel.[25−27] Numerous references have reported about the use of microreactors for preparing polymers with high yield, uniform, and well-defined properties. Polymers with various structures, such as linear, star,[28] cyclic[29,30] multiblock,[31,32] and gradient polymers[33] have been synthesized in microreactors, usually exhibiting more precisely controllable molecular weights or more specific structures than those obtained from batch counterparts.[34]

One fundamental feature of branched polymers is their relatively low viscosities, which is theoretically beneficial for continuous-flow operations without clogging in the applied tubular reactors. However, in contrast to the preparation of linear polymers, the application of continuous-flow reactors for constructing polymers with branched architectures is still in an early stage. Isaure et al.[35] reported the synthesis of water-soluble branched poly(dimethyl acrylamide) in parallel tubular reactors. The tubular reactors had higher space-time yields compared to flasks, and the products were slightly different owing to the better sealing of the tubular reactors and hence superior exclusion of traces of O_2. Liu and Chang[36] synthesized dendritic poly(amido amine) in a convergent multistep microreactor system based on an individually designed setup with an interdigital micromixer. The reaction time of each step was reduced from several hours to seconds at room temperature instead of 0 °C required for batch reactors. Wilms et al.[37] realized the ring-opening multibranched polymerization of glycidol in a microfluidic device. Such an exothermic reaction benefited from the fast heat and mass transfer provided by microreactors, meanwhile avoiding the time-consuming monomer addition in the batch operation. Combining atom transfer radical polymerization with SCVP, Bally et al.[38] reported the synthesis of branched poly(methyl methacrylate) in microreactors. Their results indicated that poly(methyl methacrylate) prepared in microreactors exhibited higher branching efficiency than batch reactors. Moreover, the coil flow inversion was applied to further reduce the mass transport limitation rising from the increased viscosity at a high monomer conversion. The improvement on the branching efficiency confirmed the effectiveness of this continuous-flow synthesis approach in controlling polymer properties.[39] Recently, Eckardt et al.[40] reported the synthesis of branched poly(butyl acrylate) (b-PBA) in a photomicroreactor with homogenous irradiation. Polymer products were synthesized under solvent-free conditions with full monomer conversion within 20 min, and stable product quality could be maintained in 24 h of continuous operation.

In this work, the synthesis of b-PBA was realized in a capillary microreactor using the Strathclyde method. The effects of branching agent divinylbenzene (DVB) and chain transfer agent dodecanethiol (DDT) on the monomer conversion, the viscosity of reaction mixture, as well as the molecular weight distribution (MWD) and the branching degree of polymer products were investigated in detail. Branching polymerization in the batch operation was also performed for comparison. It was demonstrated that better molecular weight control and higher branching degree were achieved in the continuous-flow processing. Besides, mini-emulsion polymerization utilizing a similar recipe was conducted in the microreactor, revealing higher polymerization rate and lower viscosity, which would extend the applicability of this continuous method in aqueous systems.

2. EXPERIMENTAL SECTION

2.1. Materials and Apparatus. Butyl acrylate (BA, AR, Sinopharm) was washed with sodium hydroxide aqueous solution (10 wt %) to remove the inhibitor and dried with 4A molecular sieves (Sinopharm). 2,2′-Azobisisobutyronitrile (AIBN, 98 wt %, Acros), DVB (80 wt % mixture of isomers, Aladdin), DDT (99 wt %, Aladdin), and toluene (AR, Sinopharm) were employed for solution polymerization as the thermal initiator, the branching agent, the chain transfer agent, and the solvent without purification. For miniemulsion polymerization, sodium dodecyl sulfate (SDS, AR, Sinopharm), hexadecane (HD, 99 wt %, Aladdin), and potassium persulfate (AR, Sinopharm) were respectively employed as the emulsifier, the co-stabilizer, and the thermal initiator without purification.

Figure 1 shows the schematic diagram of the experimental setup for synthesizing PBA. The capillary microreactor was

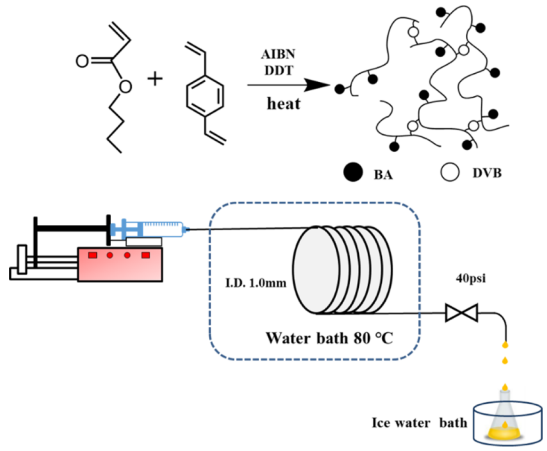

Figure 1. Schematic overview of the microreactor system for the synthesis of b-PBA.

composed of a perfluoroalkoxy (PFA) tubing (IDEX Health & Science) with 1 mm inner diameter and 5.2 m length. A high-pressure syringe pump (New Era Pump System, NE-1200) was applied to introduce the reaction mixture into the microreactor. A 40 psi backpressure regulator was positioned inline after the microreactor to prevent solvent loss from evaporation. The microreactor system was immersed in a water bath to maintain a set temperature.

2.2. Synthesis Procedure for Continuous Solution Polymerization. For all polymerization processes, the content of monomers in the reaction mixture was 30 wt %. A homogeneous solution was prepared by adding AIBN, DVB, DDT, and toluene into a dried flask sealed with a rubber septum, and then purging by N_2 for 30 min. The microreactor was flushed with dry toluene to purge moisture and oxygen existing inside the system. Then, the reaction mixture was introduced into the microreactor system by a syringe pump. After the flow inside the capillary reached a stable state, the effluent from the microreactor outlet was collected by a sample vial immersed in the ice water mixture to rapidly quench the polymerization process. The composition of the b-PBA could be controlled by changing the molar contents of the branching agent and the chain transfer agent, which were represented by the recipe of BA_{100}−DVB_m−DDT_n (the subscripts m and n denote the DVB and DDT mole dosages compared to BA, and the molar ratio of AIBN to BA was kept at 1%). The

DOI: 10.1021/acs.iecr.9b03906
Ind. Eng. Chem. Res. 2019, 58, 21312−21322

polymerization procedure for preparing linear PBA (l-PBA) was similar to that of b-PBA but without the use of the branching agent DVB.

2.3. Synthesis Procedure for Batch Solution Polymerization. The synthesis of b-PBA was carried out in a 50 mL flask for comparison. The reaction mixture was prepared following the same procedure in the continuous way. Then, the flask containing the reactants was immersed in a water bath controlled at 80 °C, with intense agitation by magnetic stirring. Samples were taken from the flask at specified time intervals and quenched immediately by the ice water mixture. Then, they were dried at 80 °C for 12 h under vacuum to remove residual monomer and toluene.

2.4. Synthesis Procedure for Continuous Miniemulsion Polymerization. The organic phase was prepared by magnetically mixing BA, DVB, DDT, and HD (2 wt % of monomers) for 10 min. The aqueous phase was formed by mixing water and SDS (5 wt % of monomers) for 10 min. The emulsion mixture was formed by adding the organic phase to the aqueous phase with magnetic stirring for 10 min, and then was homogenized at 13 000 rpm for 5 min using a high shear device (Fluko FA28 model) immersed in an ice water bath. The miniemulsion was transferred to a dried flask, and the following operations like deoxygenation and injection to the PFA capillary microreactor were similar to those in the continuous solution polymerization.

2.5. Characterization. The monomer conversion was determined gravimetrically. Chemical structures of polymer products were characterized by ^{1}H NMR spectra recorded on a 400 MHz spectrometer with $CDCl_3$ as the solvent and Fourier transform infrared (FT-IR) spectra recorded on a Thermo Nicolet 470 spectrometer. The viscosity of the reaction mixture after polymerization (i.e., the polymer solution) was measured by a viscometer (DV2T, Brookfield, USA) at 25 °C. The particle size of the latex sample in miniemulsion polymerization was measured with a laser diffraction particle size analyzer (Mastersizer-3000, Malvern, UK). The molecular weight properties of polymer products including number-average molecular weight (M_n), weight-average molecular weight (M_w), and dispersity ($Đ = M_w/M_n$) were measured using an integrated Tosoh EcoSEC GPC System including a Waters 2414 refractive index (RI) detector, a multiangle laser light scattering (LS) detector (DAWN EOS, Wyatt Technology) and a Wyatt ViscoStar II viscometer detector (DP). The GPC characterization was conducted at 40 °C with HPLC-grade tetrahydrofuran (THF) as a mobile phase at a flow rate of 1.0 mL/min. Seven narrow polystyrene standards (molecular weights from 500 to 2 110 000 g/mol) were used for calibration. An RI increment (dn/dc) of 0.065 was used for LS detection.

3. RESULTS AND DISCUSSION

3.1. PBA Products with Different Structures Prepared in the Microreactor. A typical ^{1}H NMR of b-PBA is shown in Figure 2a. The DDT residues are visible at 2.48 ppm and the broad aromatic H signal because of the DVB residues is manifested at 7.00 ppm. Figure 2b shows the FT-IR difference between l-PBA and b-PBA, and the signal at 1625 cm^{-1} relating to the stretching vibration absorption peak[41] of benzene ring skeleton proves the incorporation of the DVB unit into b-PBA.

PBA products with different structures were prepared in the microreactor by adjusting the feeding recipe. For the recipe of

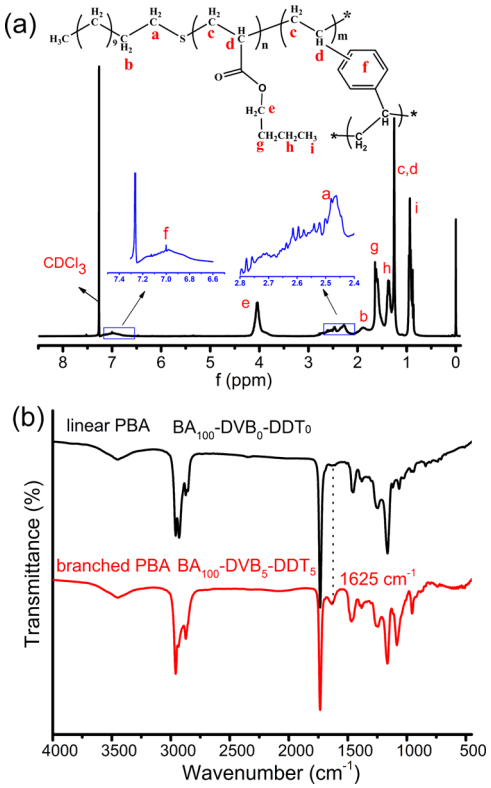

Figure 2. ^{1}H NMR spectrum (a) and FT-IR spectra (b) of b-PBA prepared in the microreactor from the recipe of BA_{100}−DVB_5−DDT_5.

BA_{100}−DVB_m−DDT_n, l-PBA was obtained without the use of DVB ($m = 0$) and cross-linked PBA was obtained without the use of DDT ($m \neq 0$ & $n = 0$). The molecular weight and branching degree of b-PBA ($m \neq 0$ & $n \neq 0$) depended on the amounts of DDT and DVB relative to BA. However, it should be noted that the excessive use of DVB would still lead to cross-linked products. Although sharing many similarities, branching and cross-linked polymer products have an essential difference as the former is free of gel formation, whereas the latter further progresses beyond the gel point for gelation. As seen in Figure 3a,b, the recipe of BA_{100}−DVB_0−DDT_2 exhibited the highest monomer conversion and the lowest viscosity of polymer solution. Compared to the conventional free radical polymerization (FRP, i.e., the recipe of BA_{100}−DVB_0−DDT_0), the chain transfer because of the use of DDT played an important role for BA_{100}−DVB_0−DDT_2, resulting in shorter polymer chains and thus reducing the average molecular weight and the chain entanglement effect. The branched structure of the polymer product was formed because of the incorporation of DVB, which was essentially a complex network of linear chains connected via a number of difunctional groups. However, without the addition of DDT, the reaction became out of control when the monomer conversion exceeded 58% with the residence time longer than 20 min, accompanied with the rise of the polymer solution viscosity above 210 cP (Figure 3b). In this case, the gel would be produced, and the pressure drop could become very high, leading to the blockage in the capillary microreactor. Interestingly, b-PBA instead of a cross-linked polymer could be smoothly obtained when an appropriate amount of chain transfer agent was applied as in the recipe of BA_{100}−DVB_1−DDT_1. For BA_{100}−DVB_1−DDT_0 with the monomer conversion of 58%, the polymer product was dissolved in THF to

DOI: 10.1021/acs.iecr.9b03906
Ind. Eng. Chem. Res. 2019, 58, 21312−21322

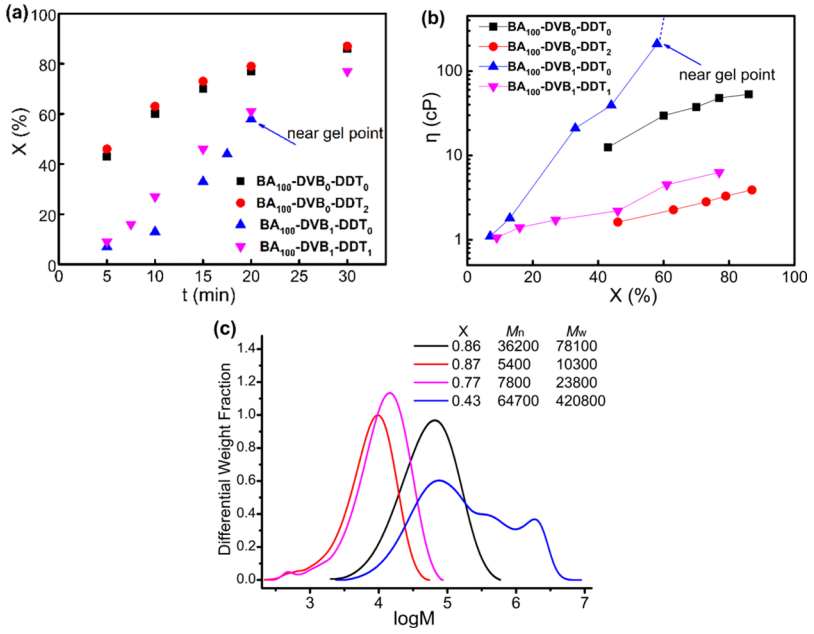

Figure 3. Monomer conversion vs residence time (a), viscosity of the polymer solution vs monomer conversion (b), and GPC traces (RI) (c) of PBA samples collected from the microreactor.

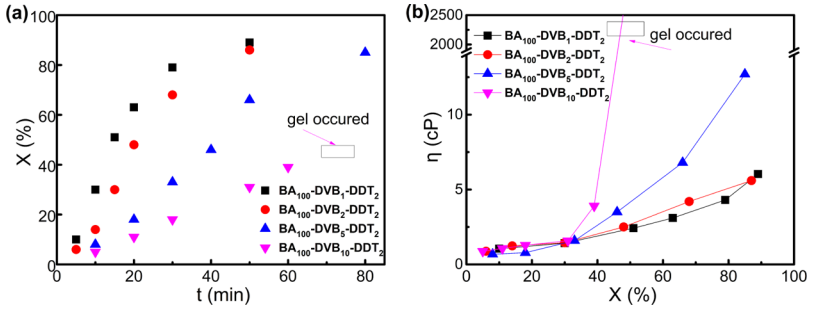

Figure 4. Monomer conversion vs residence time (a) and viscosity of the polymer solution vs monomer conversion (b) of PBA samples collected from the microreactor.

prepare a sample with the concentration of 5 mg/mL for the GPC measurement. However, such a sample failed to pass through a PTFE filter with 0.22 μm pore size because of strong resistance, indicating the formation of microgel in this seemingly homogeneous solution. The highly cross-linked microgel at the microscopic level would tend to be further interconnected through intermolecular reactions, eventually forming a gel network on a macroscopic scale. In particular, the cross-linked polymer product of BA_{100}−DVB_1−DDT_0 with the monomer conversion of 43% exhibited the highest dispersity value ($Đ$ = 6.5) among the four involved recipes, which was in consistence with the appearance of several shoulder peaks in the MWD curve (Figure 3c). This was mainly attributed to the cross-linking process that occurred unevenly.

3.2. Effects of the Dosages of DVB and DDT on b-PBA in the Microreactor. DVB functioned as a branching agent and served as a comonomer along with BA. The primary chain length was controlled by the proportion of DDT, which introduced the chain transfer reaction and suppressed the gelation process, therefore facilitating the synthesis of branched polymer products. The effects of the DVB and DDT dosages on the branched polymerization process were investigated in detail.

As seen in Figure 4, the decrease in the reaction rate and the increase in the viscosity of the polymer solution were observed when the DVB amount rose. As DVB used in this work was a mixture of three isomers, the kinetic data such as reactivity ratio and the chain propagation rate were hard to determine. However, considering that the structure of DVB was similar to that of styrene, and the latter had lower chain propagation rate and higher reactivity ratio than BA, DVB was thought to be consumed faster in the copolymerization process. For the recipe of BA_{100}−DVB_{10}−DDT_2, DVB was overdosed, and thus a highly branched oligomer could be formed even at the early polymerization stage (Figure 4a). With insufficient DDT, the gel network with infinitely large molecular weight tended to be formed after the monomer conversion reached 40%, and the viscosity would rise sharply from 3.9 cP to several thousand cP (Figure 4b). Moreover, the chain propagation rate would get slower as the segmental movement in the high-viscosity reaction mixture was hindered with the monomer conversion raising. When the amount of DDT was increased and that of DVB was maintained constant, the viscosity of the polymer solution slightly dropped down (see Supporting Information Figure S1b). The mobility of the polymer chain would be weakly affected as the reaction systems were in low viscosity (below 20 cP), and the monomer conversion was almost kept

DOI: 10.1021/acs.iecr.9b03906
Ind. Eng. Chem. Res. 2019, 58, 21312−21322

Table 1. Summary of Polymerization Conditions and Characterization of PBA Samples

sample[a]	feed ratio (mol) BA−DVB−DDT	t (min)	X (%)	M_n[b] (kg/mol)	M_w[b] (kg/mol)	$Đ$[b]	$M_{n,LS}$[c] (kg/mol)	$M_{w,LS}$[c] (kg/mol)	α[d]
1[e]	100/0/0	30	86	36.2	78.1	2.1	46.6	79.1	0.71
2	100/1/2	50	89	6.9	16.3	2.4	10.2	18.6	0.58
3	100/2/2	50	87	7.9	20.4	2.6	12.6	22.7	0.51
4	100/5/2	80	85	12.4	111.3	9.0	29.2	182.4	0.46
5	100/1/0.3	50	85	20.9	98.5	4.7	30.3	111.6	0.65
6	100/1/0.5	50	85	15.7	65.0	4.1	25.9	60.1	0.64
7	100/1/1	30	77	10.8	23.8	2.2	24.3	38.0	0.60
8	100/5/5	80	88	5.9	15.3	2.6	11.5	26.1	0.45
9	100/10/10	80	89	4.4	11.7	2.7	13.2	20.3	0.42

[a]Polymer samples were collected in the corresponding residence time at a steady state. [b]M_n, M_w, and $Đ$ were measured by the differential RI detector. [c]$M_{n,LS}$ and $M_{w,LS}$ were measured by the multiangle laser LS detector. [d]The Mark−Houwink exponent α was determined by the viscometer (DP) detector. [e]Run 1 was a l-PBA sample.

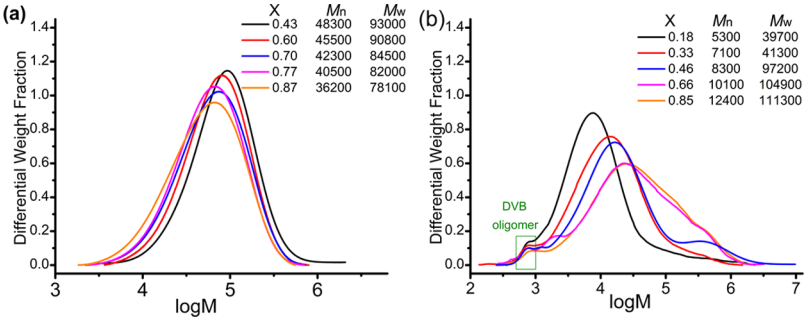

Figure 5. GPC traces (RI) of PBA samples collected from the microreactor with different recipes along with monomer conversion: (a) BA_{100}−DVB_0−DDT_0; (b) BA_{100}−DVB_5−DDT_2.

the same with the variation of DDT amount for varied residence times (Figure S1a). Such results were expected as DDT solely acted as a chain transfer agent and its amount should have no obvious effect on the concentration of radical chains.[41] When both the DDT and DVB dosages were increased simultaneously at the molar ratio of 1:1, the monomer conversion gradually decreased because of the participation of more DVB molecules in the copolymerization (Figure S1c). Moreover, the overall chain propagation rate became slower, and the polymer solution viscosity was kept below 10 cP even at the monomer conversion of 85% (Figure S1d). Such a viscosity was obviously lower than that for the FRP recipe (i.e., 45 cP), owing to the formation of the branched structure.

Polymer products with various branching degrees were analyzed by triple-detection gel permeation chromatography. Table 1 and Figure S2 show the molecular weight results for the samples at the highest monomer conversion using the aforementioned recipes. The prepared b-PBA samples had M_n of 4.4−20.9 kg/mol and $Đ$ of 2.2−9.0. Both M_n and $Đ$ increased at a higher DVB concentration (Figure S2a). In contrast, they decreased with increasing the amount of DDT (Figure S2c). This was because the length of the primary chain became shorter and the branching process occurred more uniformly, restricting the formation of larger molecules. $M_{n,LS}$ and $M_{w,LS}$ also showed similar trends with regard to the effects of DVB and DDT dosages (Table 1).

The branching degree is generally described by the mean-square radius of gyration through the LS detection or by the intrinsic viscosity through the DP detection. As the mean square radius of gyration was beyond the detectability of LS detection[42] (the values of $M_{n,LS}$ for some samples in our case were lower than 20 kg/mol), DP detection was employed to generate Mark−Houwink plots ($M = K[\eta]^{\alpha}$, where M is the molecular weight, $[\eta]$ is the intrinsic viscosity with K and α as constants). The b-PBA sample with a lower intrinsic viscosity at the same molecular weight was considered to own a higher branching degree. The branching degree can also be characterized by the values of α (the Mark−Houwink exponent) derived from the slopes of these plots. As shown in Table 1, the l-PBA in sample 1 gave a measured α value of 0.71, which was close to the literature value of 0.7.[40] For other samples, the α values were lower, suggesting densely packed three-dimensional structures. In samples 5−7, the values of α were quite close to each other but slightly decreased with increasing the DDT content (Figure S2d). As expected, introducing DVB into the polymer product was beneficial for increasing the number of branched units. Also, for the H-type branched unit composed of two T-type branching points[43] (Figure S3), the introduction of one DVB unit required to consume two DDT units as end groups to prevent being excessively cross-linked during the polymerization process. When the DDT amount was insufficient, the number of H-type branched unit decreased, hence the branching degree was lowered. In such cases, the hindrance effect of the chain entanglement was enhanced, resulting in the increase of the polymer solution viscosity (Figure S1b).

3.3. Understanding the Branched Polymerization Process Based on Molecular Weight Development. In the previous part, the effect of the feeding recipe on the final PBA was mainly analyzed with the monomer conversion between 80 and 90%. It would take a rather long operation time to reach higher monomer conversions and meanwhile gelation might occur. To prepare the branched polymers free of the gelation and even with controlled branched structures, understanding the branching process would be of guidance.

DOI: 10.1021/acs.iecr.9b03906
Ind. Eng. Chem. Res. 2019, 58, 21312−21322

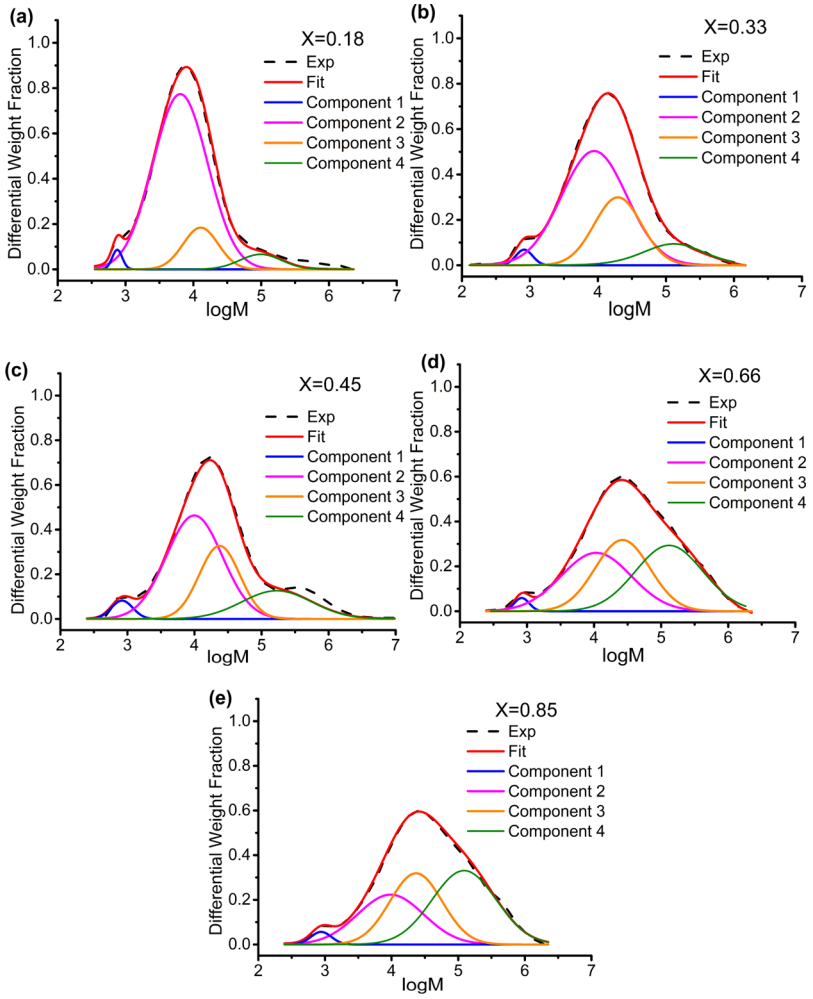

Figure 6. Deconvolution of the multimodal MWDs of the b-PBA samples collected from the microreactor for the recipe of BA_{100}−DVB_5−DDT_2 at different monomer conversions: (a) X = 0.18, (b) X = 0.33, (c) X = 0.45, (d) X = 0.66, (e) X = 0.85.

Table 2. Deconvolution Results of the b-PBA Samples of Recipe BA_{100}−DVB_5−DDT_2

	X = 0.18		X = 0.33		X = 0.45		X = 0.66		X = 0.85	
component	[a]$M_p \times 10^3$	[b]area	$M_p \times 10^3$	area	$M_p \times 10^3$	area	$M_p \times 10^3$	area	$M_p \times 10^3$	area
1	0.8	0.02	0.8	0.02	0.8	0.02	0.8	0.02	0.9	0.02
2	6.4	0.8	8.9	0.6	9.9	0.51	10.6	0.33	9.7	0.26
3	12.8	0.13	19.2	0.26	23.6	0.28	25.3	0.33	24.3	0.32
4	98.4	0.05	108.4	0.12	168.2	0.18	161.8	0.32	155.0	0.4

[a]M_p = the peak molecular weight of the component. [b]Area = the weight fraction of the component.

Here, we collected samples at various monomer conversions for the recipe of BA_{100}−DVB_5−DDT_2 and the development of the corresponding MWDs was used to explain the branching process.

Figure 5 shows the evolution of MWD curves of l-PBA and b-PBA prepared in the microreactor. For the recipe of BA_{100}−DVB_0−DDT_0, M_n decreased with the increase of the monomer conversion (Figure 5a), and $Đ$ was maintained at around 2.0. In contrast, for the recipe of BA_{100}−DVB_5−DDT_2, both M_n and M_w increased gradually with the polymerization processing. In Figure 5b, there were small shoulder peaks of the MWD curves at low molecular weight regions (<1000 g/mol), which was attributed to a low proportion of DVB oligomers. At the early polymerization stage, DVB was consumed quickly and might be transformed into homopolymer with several structural units. Compared to BA oligomers, DVB oligomers had lower chain mobility, and their incorporation into the main branched structure would be impeded by steric hindrance. Eventually, the DVB oligomers were subjected to the early termination and accumulated as dead chains with low molecular weights. Also, from Figure S2a, it can be found that the more DVB was used, the higher proportion of the oligomer component was occupied.

In contrast to l-PBA samples, all GPC traces (RI) of b-PBA samples (Figure 5b) show multimodal MWDs overlaid by several unimodal distribution peaks, indicating polymer chain components of different molecular weights. Inspired by Yang's[44] and McEwan's[45] works, the MWDs are deconvoluted into several unimodal subpopulations to get quantitative information to understand the branched polymerization

DOI: 10.1021/acs.iecr.9b03906
Ind. Eng. Chem. Res. 2019, 58, 21312−21322

process. Generally, the Gaussian distribution has the best correlation with most of unimodal polymer MWDs. For convenience, we applied four Gaussian distribution peaks to represent subpopulations of these polymer chain components. With the molecular weight increasing, component 1 represents the DVB oligomers, whereas components 2, 3, and 4 are considered to be related to the primary chains, the slightly branched chains consisting of two primary chain units and the highly branched chains containing more than three primary chain units, respectively. The sum of the weight fraction (w_i) of these four components equals 1, that is, $\sum w_i = 1$ (i = 1, 2, 3, 4). PeakFit v4 software was applied to perform the deconvolution, and the results for the multimodal MWDs are shown in Figure 6.

The agreements between the experimental and fitted MWDs appeared good with R^2 value over 0.99. As seen in Table 2, because of the existence of both the chain transfer and the chain propagation, the molecular weights of components 2 and 3 increased throughout the reaction, and the peak molecular weight of component 3 ($M_{p,3}$) was approximately two times that of $M_{p,2}$ at the same monomer conversion, in accordance with our assumption that component 3 consisted of two primary chains. $M_{p,4}$ was much bigger than $M_{p,3}$, suggesting that the formation of component 4 was very complex, including not only the coupling products of slightly branched chains from component 3, but also the coupling products of itself with primary chains and slightly branched chains from components 2 and 3.

Figure 7 shows the evolution of the weight fraction of every component. The weight fraction of component 1 (w_1) was

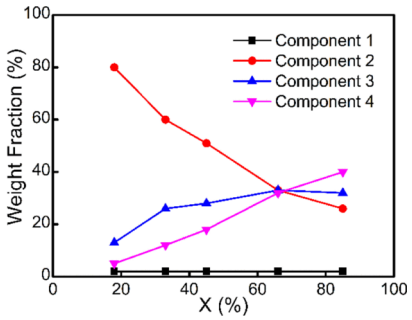

Figure 7. Variation of the weight fraction of the four components deconvoluted from multimodal MWDs at different monomer conversions.

kept at a tiny value below 0.02 because of the low mobility of DVB oligomers during the whole process. Whereas w_2 decreased continuously, w_3 first increased to a maximum value around 0.33 and then decreased, because slightly branched chains were consumed more than those obtained from the coupling of two primary chains after the monomer conversion reached a certain value. Accordingly, w_4 rose with the increase of the monomer conversion as highly branched chains were accumulated from the early stage of the polymerization. Yet, w_4 was rather low at the monomer conversion of 18%. Moreover, the coupling reaction between highly branched chains would become more dominant at the later polymerization stage, giving rise to the formation of large and highly branched chains accompanied with the increase in the molecular weight and in the dispersity. Whereas the polymer solution was in low viscosity of 12.7 cP at the monomer conversion of 85% (Figure 4b), w_4 would continue to increase according to the trend in Figure 7 until the polymerization system approached the instantaneous gel point. Therefore, the risk of gelation still exists for the recipe of BA_{100}−DVB_5−DDT_2, and residence time should be adjusted to avoid the cross-linking by terminating polymerization in advance.

In all, the analysis of MWD curves at various monomer conversions revealed the gradual branching process, as the weight fractions of components with different branching degrees kept changing. In the early polymerization stage, small and slightly branched chains were formed from the coupling reaction between primary chains. While in the later stage, the coupling between branched chains would become dominant, resulting in the large and highly branched chains with the increase of both molecular weight and dispersity. Still, further work is needed to predict the gel point in the continuous-flow system.

3.4. Comparison of the Branched Polymerization Performance between Microreactors and Batch Reactors. The comparison between the capillary microreactor and the batch reactor for the preparation of b-PBA is presented in Figure 8, using the recipe of BA_{100}−DVB_5−DDT_2. It can be seen that the polymerization was initiated quickly in the microreactor (Figure 8a), owing to its enhanced heat and mass transfer. The reaction mixture could be quickly heated to the set temperature upon entering the microreactor, and the generated free radicals would rapidly contact with monomers to propagate in the narrow confined channel. Instead, it would take a longer time to reach the set reaction temperature in the batch reactor, and the temperature variation of the reaction mixture could reach 5.5 °C, with the temperature being higher than that of the external heating source (Figure S5a). For the continuous process, owing to the small diameter of the capillary microreactor, it was hard to directly insert a temperature sensor into the inside solution. Therefore, a heat transfer model was utilized to analyze the temperature distribution inside the microreactor and the temperature variation was calculated to be below 0.1 °C (Figure S5b).

Because of the exothermic polymerization, the produced heat was accumulated in the batch reactor and thus the reaction was accelerated. The batch operation had higher conversion after the reaction time of 40 min compared to the continuous-flow processing (Figure 8a). In particular, for the recipe of BA_{100}−DVB_0−DDT_0 to prepare l-PBA, the higher the polymerization heat production rate was, the worse temperature control would be in the batch reactor. In this case, $Đ$ was 3.4 in the batch operation, larger than that of 2.1 in the microreactor (Figure S6a). Such a low dispersity value obtained from the continuous operation was similar to Iwasaki's report,[46] as the microreactor was suitable for the MWD control in highly exothermic systems.

Moreover, the Mark−Houwink plots of l-PBA samples from batch and continuous operations overlapped at the molecular weight region below 200 kg/mol, and then the intrinsic viscosity of the l-PBA sample from the flask was clearly lower than that from the microreactor (Figure S6b), which might be attributed to the existence of long-chain branches in the batch process. For the polymerization of BA at high temperatures (>343 K), linear primary chains could be transformed to secondary and tertiary macroradicals because of backbiting (intramolecular chain transfer to polymer) and subsequent β-scission,[47] and the following macroradicals' propagation led to the formation of both short and long chain branches.

DOI: 10.1021/acs.iecr.9b03906
Ind. Eng. Chem. Res. 2019, 58, 21312−21322

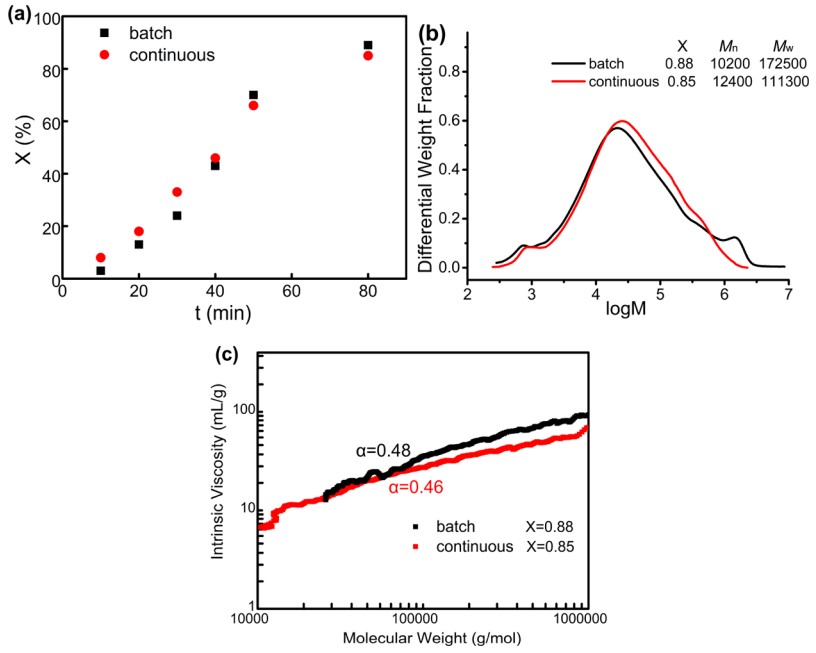

Figure 8. Characterization of the PBA samples for the recipe of BA_{100}–DVB_5–DDT_2 in batch and continuous solution polymerization: (a) monomer conversion vs residence time in the microreactor, (b) GPC traces (RI), and (c) Mark–Houwink plots.

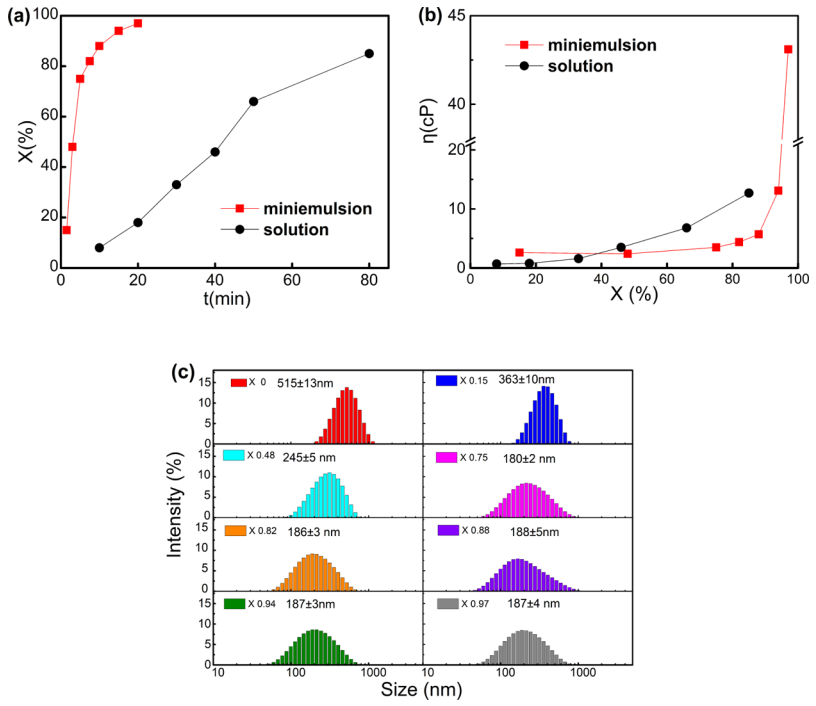

Figure 9. Characterization of the PBA samples for the recipe of BA_{100}–DVB_5–DDT_2 obtained through solution and miniemulsion polymerization in the microreactor: (a) monomer conversion vs residence time, (b) viscosity vs monomer conversion, (c) particle size distributions of latex particles vs monomer conversion in a miniemulsion system.

Intermolecular chain transfer to polymer could also cause the formation of long chain branches, and the mechanism can be seen in Figure S7.[48,49] Chain transfer agents with thiol function groups can help to suppress such side reactions.[50,51] However, both the backbiting and β-scission reactions that required high activation energy are more likely to occur in the batch system because of the local hot spots. The formation of long chain branches increased the heterogeneity of the linear primary chains, then complicated the branched structure formed with DVB as the coupling center, and eventually resulted in higher dispersity of the polymer product for the batch processing. As shown in Figure 8b, the b-PBA sample prepared in the batch reactor with the monomer conversion of 88% exhibited lower M_n and higher M_w compared to the sample from the microreactor at the comparable conversion of 85%.

Such irregular branches in primary chains were supposed to increase the branching degree of b-PBA samples from the batch reactor. However, the polymer product from the batch

DOI: 10.1021/acs.iecr.9b03906
Ind. Eng. Chem. Res. 2019, 58, 21312–21322

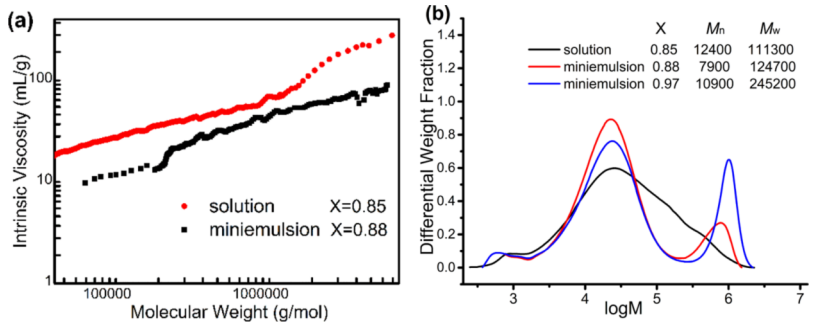

Figure 10. Characterization of the PBA samples for the recipe of BA_{100}−DVB_5−DDT_2 obtained through solution and miniemulsion polymerization in the microreactor: (a) Mark−Houwink plots; (b) GPC traces (RI).

processing showed higher intrinsic viscosity at the same molecular weight, that is, lower branching degree than that from the microreactor (Figure 8c). This could be attributed to the higher mixing efficiency in the microreactor. That is, the process from the primary chain to the slightly branched chain and then to the highly branched chain was less affected by the mass transport limitation in the microreactor, which is considered to have a pretty significant effect on the final branching degree. However, for the batch processing, the coupling reaction was restricted by the diffusion distance, which would reduce the probability of the contact between chains containing suspended double bonds. In short, the polymers prepared in the microreactor have higher branching efficiency because of the reduced diffusion pathway; meanwhile, possible side reactions such as uncontrollable branches' formation from linear primary chains are avoided benefiting from more homogeneous temperature control.

3.5. Branched Polymerization Performance under a Miniemulsion System in the Microreactor. From the aforementioned branched polymerization kinetics in a solution system, it was found that increasing the amount of branching agent was advantageous for increasing the branching degree, while sacrificing the apparent reaction rate. This dilemma was tried to be solved by utilizing the emulsion system. In emulsion polymerization, each radical is confined to a nanoparticle in the dispersed phase. This is beneficial for suppressing bimolecular termination, resulting in higher polymerization rate and molecular weight.[52] However, phase separation and coagulation are prone to happen during the emulsion polymerization in tubular reactors without continuous stirring.[53] We turned to utilize the high shear device, as the monomer phase in the preemulsion was further broken up, with the diameter of dispersed droplets to submicron level, resulting in stable miniemulsion systems for the following polymerization in microreactors.[54] In our case, the prepared miniemulsion could be stored for at least 2 months without sedimentation or phase separation.

Taking the recipe of BA_{100}−DVB_5−DDT_2 for example, as shown in Figure 9a, the miniemulsion polymerization took only 15 min to reach over 90% monomer conversion, which was significantly faster than the solution polymerization. Also, the viscosity in the miniemulsion system was lower (Figure 9b), with the viscosity of the output latex below 45 cP even at the monomer conversion of 97%. The blockage happened when the residence time was prolonged to 30 min, indicating that the miniemulsion system was close to the gel point, which was, however, delayed at a very high monomer conversion (>99%). The particle size distribution for all latex samples was unimodal (Figure 9c), and the volume-weighted mean particle size first decreased from 515 nm to around 180 nm and then went steady with the increase of the monomer conversion. In ideal miniemulsion polymerization, monomer droplets are totally nucleated into particles, and the particle size is assumed to be uniform. However, in our situation, homogeneous nucleation may exist and once heated, the monomer from the large droplets would diffuse into the continuous aqueous phase in the initial stage, and then capture the free radicals to form new latex particles. The increase in the number of latex particles corresponded to the reduction of the particle size. With the reaction proceeding, hydrophobic polymer chains formed could act as co-stabilizers with HD to retard the monomer diffusion, so the particle size turned steady from a certain moment.

The formation of a gel network in the miniemulsion system would not be easy as that in the solution system, resulting in lower viscosity. DVB and BA monomers initially resided within the nanometer-scale droplets. At the early reaction stage, the confined space inside the latex particles forced primary chains to contact with each other for effective branching. The subsequent coupling reaction between polymer chains bearing the suspended double bonds was also benefited from the short diffusion pathway. The branching efficiency was therefore improved, and the intrinsic viscosities of polymer products from the miniemulsion polymerization were lower (Figure 10a). However, $Đ$ of the polymer product from the miniemulsion polymerization was larger than that from the solution polymerization at a comparable conversion of 85%. This could be demonstrated by the GPC trace with a distinct shoulder peak in a high molecular weight region (around 10^6 g/mol) for the miniemulsion polymerization, and the weight fraction of that peak became larger at the conversion of 97% (Figure 10b). The uneven MWD with two peaks separated obviously was highly possible related to the heterogeneous particle size distribution, as branched polymer products with higher molecular weight were obtained in larger dispersed droplets, and vice versa. In summary, the miniemulsion polymerization in the microreactor seems quite promising to synthesize branched polymer products, with the high shear devices commercially available applied for the preparation of miniemulsion.

4. CONCLUSIONS

In this work, a capillary microreactor was employed for the synthesis of b-PBA using the Strathclyde method. This continuous process was convenient to generate PBA with different structures by adjusting the branching agent DVB and chain transfer agent DDT dosages and the flow rate. A detailed

DOI: 10.1021/acs.iecr.9b03906
Ind. Eng. Chem. Res. 2019, 58, 21312−21322

analysis regarding the effect of the polymerization recipe on the preparation of b-PBA was made, as more DVB brought higher branching degree and DDT was required to inhibit the gel occurrence. MWDs of b-PBA along with the monomer conversion were multimodal and they were deconvoluted to reveal the gradual branching process. The increase of the branching degree for b-PBA was reached with the continuous-flow processing, owing to better heat and mass transport capacities in the microreactor compared to the batch reactor. Moreover, the continuous synthesis of b-PBA was promising in aqueous miniemulsion polymerization, exhibiting higher reaction rate, lower solution viscosity, and improved branching degree. This work demonstrated that commercially available monomers could be directly applied to continuously prepare branched polymers with high branching efficiency in microreactors under mild conditions utilizing the Strathclyde method.

■ ASSOCIATED CONTENT

Supporting Information

The Supporting Information is available free of charge on the ACS Publications website at DOI: 10.1021/acs.iecr.9b03906.

Further information on the polymerization kinetics of BA, the heat transfer analysis for the microreactor, and the mechanism of side reactions (PDF)

■ AUTHOR INFORMATION

Corresponding Author

*E-mail: y.su@sjtu.edu.cn. Phone: +86 21-54738710.

ORCID

Yuanhai Su: 0000-0002-0718-301X

Notes

The authors declare no competing financial interest.

■ ACKNOWLEDGMENTS

We would like to acknowledge financial support from the National Natural Science Foundation of China (no. 21676164) and the Science and Technology Commission of Shanghai Municipality (no. 18520743500). We also thank Chong Shen for his help in dealing with some experimental data.

■ REFERENCES

(1) Flory, P. J. Molecular Size Distribution in Three Dimensional Polymers. VI. Branched Polymers Containing A−R−B_{f-1} Type Units. *J. Am. Chem. Soc.* **1952**, *74*, 2718−2723.

(2) Kim, Y. H. Lyotropic liquid crystalline hyperbranched aromatic polyamides. *J. Am. Chem. Soc.* **1992**, *114*, 4947−4948.

(3) England, R. M.; Rimmer, S. Hyper/highly-branched polymers by radical polymerisations. *Polym. Chem.* **2010**, *1*, 1533−1544.

(4) Zhu, X.; Zhou, Y.; Yan, D. Influence of Branching Architecture on Polymer Properties. *J. Polym. Sci., Part B: Polym. Phys.* **2011**, *49*, 1277−1286.

(5) Slark, A. T.; Sherrington, D. C.; Titterton, A.; Martin, I. K. Branched methacrylate copolymers from multifunctional comonomers: the effect of multifunctional monomer functionality on polymer architecture and properties. *J. Mater. Chem.* **2003**, *13*, 2711−2720.

(6) Voit, B. New developments in hyperbranched polymers. *J. Polym. Sci., Part A: Polym. Chem.* **2000**, *38*, 2505−2525.

(7) Wang, D.; Wang, W.-J.; Li, B.-G.; Zhu, S. Semibatch RAFT Polymerization for Branched Polyacrylamide Production: Effect of Divinyl Monomer Feeding Policies. *AIChE J.* **2013**, *59*, 1322−1333.

(8) Hong, Y.; Coombs, S. J.; Cooper-White, J. J.; Mackay, M. E.; Hawker, C. J.; Malmström, E.; Rehnberg, N. Film blowing of linear low-density polyethylene blended with a novel hyperbranched polymer processing aid. *Polymer* **2000**, *41*, 7705−7713.

(9) Liu, P.; Ye, Z.; Wang, W.-J.; Li, B.-G. Hyperbranched Polyethylenes Encapsulating Self-Supported Palladium(II) Species as Efficient and Recyclable Catalysts for Heck Reaction. *Macromolecules* **2012**, *46*, 72−82.

(10) Song, L.; Tu, C.; Shi, Y.; Qiu, F.; He, L.; Jiang, Y.; Zhu, Q.; Zhu, B.; Yan, D.; Zhu, X. Controlling the Optical Properties of Hyperbranched Conjugated Polyazomethines through Terminal-Backbone Interactions. *Macromol. Rapid Commun.* **2010**, *31*, 443−448.

(11) Shepherd, J.; Sarker, P.; Swindells, K.; Douglas, I.; MacNeil, S.; Swanson, L.; Rimmer, S. Binding bacteria to highly branched poly(*N*-isopropyl acrylamide) modified with vancomycin induces the coil-to-globule transition. *J. Am. Chem. Soc.* **2010**, *132*, 1736−1737.

(12) Wang, Y.; Grayson, S. M. Approaches for the preparation of non-linear amphiphilic polymers and their applications to drug delivery. *Adv. Drug Delivery Rev.* **2012**, *64*, 852−865.

(13) Hawker, C. J.; Lee, R.; Frechet, J. M. J. One-Step Synthesis of Hyperbranched Dendritic Polyesters. *J. Am. Chem. Soc.* **1991**, *113*, 4583−4588.

(14) Emrick, T.; Chang, H.-T.; Fréchet, J. M. J. An A_2 + B_3 Approach to Hyperbranched Aliphatic Polyethers Containing Chain End Epoxy Substituents. *Macromolecules* **1999**, *32*, 6380−6382.

(15) Voit, B. I.; Lederer, A. Hyperbranched and Highly Branched Polymer Architectures—Synthetic Strategies and Major Characterization Aspects. *Chem. Rev.* **2009**, *109*, 5924−5973.

(16) Frechet, J. M. J.; Henmi, M.; Gitsov, I.; Aoshima, S.; Leduc, M. R.; Grubbs, R. B. Self-condensing vinyl polymerization: an approach to dendritic materials. *Science* **1995**, *269*, 1080−1083.

(17) Wang, W.-J.; Wang, D.; Li, B.-G.; Zhu, S. Synthesis and Characterization of Hyperbranched Polyacrylamide Using Semibatch Reversible Addition−Fragmentation Chain Transfer (RAFT) Polymerization. *Macromolecules* **2010**, *43*, 4062−4069.

(18) Bally, F.; Ismailova, E.; Brochon, C.; Serra, C. A.; Hadziioannou, G. Mechanistic study of Atom Transfer Radical Polymerization in the Presence of an Inimer: Toward Highly Branched Controlled Macromolecular Architectures through One-Pot Reaction. *Macromolecules* **2011**, *44*, 7124−7131.

(19) Li, F.; Cao, M.; Feng, Y.; Liang, R.; Fu, X.; Zhong, M. Site-Specifically Initiated Controlled/Living Branching Radical Polymerization: A Synthetic Route toward Hierarchically Branched Architectures. *J. Am. Chem. Soc.* **2019**, *141*, 794−799.

(20) Baudry, R.; Sherrington, D. C. Synthesis of Highly Branched Poly(methyl methacrylate)s Using the "Strathclyde Methodology" in Aqueous Emulsion. *Macromolecules* **2006**, *39*, 1455−1460.

(21) Jiang, L.; Huang, W.; Xue, X.; Yang, H.; Jiang, B.; Zhang, D.; Fang, J.; Chen, J.; Yang, Y.; Zhai, G.; Kong, L.; Wang, S. Radical Polymerization in the Presence of Chain Transfer Monomer: An Approach to Branched Vinyl Polymers. *Macromolecules* **2012**, *45*, 4092−4100.

(22) Huang, W.; Li, J.; Wu, H.; Ren, Z.; Wang, S.; Jiang, Q.; Xue, X.; Yang, H.; Jiang, B.; Chen, J. Preparation of branched polystyrene by free radical emulsion polymerization in the presence of functional monomer. *Mater. Res. Innovations* **2018**, *22*, 379−384.

(23) Costello, P. A.; Martin, I. K.; Slark, A. T.; Sherrington, D. C.; Titterton, A. Branched methacrylate copolymers from multifunctional monomers: chemical composition and physical architecture distributions. *Polymer* **2002**, *43*, 245−254.

(24) Baudry, R.; Sherrington, D. C. Facile synthesis of branched poly(vinyl alcohol)s. *Macromolecules* **2006**, *39*, 5230−5237.

(25) Iwasaki, T.; Kawano, N.; Yoshida, J.-i. Radical polymerization using microflow system: Numbering-up of microreactors and continuous operation. *Org. Process Res. Dev.* **2006**, *10*, 1126−1131.

(26) Su, Y.; Kuijpers, K.; Hessel, V.; Noël, T. A convenient numbering-up strategy for the scale-up of gas−liquid photoredox catalysis in flow. *React. Chem. Eng.* **2016**, *1*, 73−81.

DOI: 10.1021/acs.iecr.9b03906
Ind. Eng. Chem. Res. 2019, 58, 21312−21322

(27) Qiu, M.; Zha, L.; Song, Y.; Xiang, L.; Su, Y. Numbering-up of capillary microreactors for homogeneous processes and its application in free radical polymerization. *React. Chem. Eng.* **2019**, *4*, 351−361.
(28) Wenn, B.; Martens, A. C.; Chuang, Y.-M.; Gruber, J.; Junkers, T. Efficient multiblock star polymer synthesis from photo-induced copper-mediated polymerization with up to 21 arms. *Polym. Chem.* **2016**, *7*, 2720−2727.
(29) Baeten, E.; Rubens, M.; Wuest, K. N. R.; Barner-Kowollik, C.; Junkers, T. Photo-induced ring-closure via a looped flow reactor. *React. Chem. Eng.* **2017**, *2*, 826−829.
(30) Sun, P.; Liu, J. A.; Zhang, Z.; Zhang, K. Scalable preparation of cyclic polymers by the ring-closure method assisted by the continuous-flow technique. *Polym. Chem.* **2016**, *7*, 2239−2244.
(31) Baeten, E.; Haven, J. J.; Junkers, T. RAFT multiblock reactor telescoping: from monomers to tetrablock copolymers in a continuous multistage reactor cascade. *Polym. Chem.* **2017**, *8*, 3815−3824.
(32) Kuroki, A.; Martinez-Botella, I.; Hornung, C. H.; Martin, L.; Williams, E. G. L.; Locock, K. E. S.; Hartlieb, M.; Perrier, S. Looped flow RAFT polymerization for multiblock copolymer synthesis. *Polym. Chem.* **2017**, *8*, 3249−3254.
(33) Corrigan, N.; Manahan, R.; Lew, Z. T.; Yeow, J.; Xu, J.; Boyer, C. Copolymers with Controlled Molecular Weight Distributions and Compositional Gradients through Flow Polymerization. *Macromolecules* **2018**, *51*, 4553−4563.
(34) Su, Y.; Song, Y.; Xiang, L. Continuous-Flow Microreactors for Polymer Synthesis: Engineering Principles and Applications. *Top. Curr. Chem.* **2018**, *376*, 44.
(35) Isaure, F.; Cormack, P. A. G.; Sherrington, D. C. Facile synthesis of branched water-soluble poly(dimethylacrylamide)s in conventional and parallel reactors using free radical polymerisation. *React. Funct. Polym.* **2006**, *66*, 65−79.
(36) Liu, S.; Chang, C.-H. High Rate Convergent Synthesis and Deposition of Polyamide Dendrimers using a Continuous-Flow Microreactor. *Chem. Eng. Technol.* **2007**, *30*, 334−340.
(37) Wilms, D.; Nieberle, J.; Klos, J.; Löwe, H.; Frey, H. Synthesis of Hyperbranched Polyglycerol in a Continuous Flow Microreactor. *Chem. Eng. Technol.* **2007**, *30*, 1519−1524.
(38) Bally, F.; Serra, C. A.; Brochon, C.; Hadziioannou, G. Synthesis of branched polymers under continuous-flow microprocess: an improvement of the control of macromolecular architectures. *Macromol. Rapid Commun.* **2011**, *32*, 1820−1825.
(39) Parida, D.; Serra, C. A.; Garg, D. K.; Hoarau, Y.; Bally, F.; Muller, R.; Bouquey, M. Coil flow inversion as a route to control polymerization in microreactors. *Macromolecules* **2014**, *47*, 3282−3287.
(40) Eckardt, O.; Wenn, B.; Biehl, P.; Junkers, T.; Schacher, F. H. Facile photo-flow synthesis of branched poly(butyl acrylate)s. *React. Chem. Eng.* **2017**, *2*, 479−486.
(41) Sengupta, S.; Das, T.; Ghorai, U. K.; Bandyopadhyay, A. Copolymers from methyl methacrylate and butyl acrylate with hyperbranched architecture. *J. Appl. Polym. Sci.* **2017**, *134*, 45356.
(42) Liang, S.; Li, X.; Wang, W.-J.; Li, B.-G.; Zhu, S. Toward Understanding of Branching in RAFT Copolymerization of Methyl Methacrylate through a Cleavable Dimethacrylate. *Macromolecules* **2016**, *49*, 752−759.
(43) Li, X.; Wang, W.-J.; Li, B.-G.; Zhu, S. Branching in RAFT Miniemulsion Copolymerization of Styrene/Triethylene Glycol Dimethacrylate and Control of Branching Density Distribution. *Macromol. React. Eng.* **2015**, *9*, 90−99.
(44) Yang, H.-J.; Jiang, B.-B.; Huang, W.-Y.; Zhang, D.-L.; Kong, L.-Z.; Chen, J.-H.; Liu, C.-L.; Gong, F.-H.; Yu, Q.; Yang, Y. Development of Branching in Atom Transfer Radical Copolymerization of Styrene with Triethylene Glycol Dimethacrylate. *Macromolecules* **2009**, *42*, 5976−5982.
(45) McEwan, K. A.; Haddleton, D. M. Combining catalytic chain transfer polymerisation (CCTP) and thio-Michael addition: enabling the synthesis of peripherally functionalised branched polymers. *Polym. Chem.* **2011**, *2*, 1992−1999.
(46) Iwasaki, T.; Yoshida, J.-i. Free radical polymerization in microreactors. Significant improvement in molecular weight distribution control. *Macromolecules* **2005**, *38*, 1159−1163.
(47) Derboven, P.; Van Steenberge, P. H. M.; Vandenbergh, J.; Reyniers, M.-F.; Junkers, T.; D'hooge, D. R.; Marin, G. B. Improved Livingness and Control over Branching in RAFT Polymerization of Acrylates: Could Microflow Synthesis Make the Difference? *Macromol. Rapid Commun.* **2015**, *36*, 2149−2155.
(48) Ballard, N.; Hamzehlou, S.; Asua, J. M. Intermolecular transfer to polymer in the radical polymerization of n-butyl acrylate. *Macromolecules* **2016**, *49*, 5418−5426.
(49) Ballard, N.; Asua, J. M. Radical polymerization of acrylic monomers: An overview. *Prog. Polym. Sci.* **2018**, *79*, 40−60.
(50) Ballard, N.; de la Cal, J. C.; Asua, J. M. The role of chain transfer agent in reducing branching content in radical polymerization of acrylates. *Macromolecules* **2015**, *48*, 987−993.
(51) Gaborieau, M.; Koo, S. P. S.; Castignolles, P.; Junkers, T.; Barner-Kowollik, C. Reducing the degree of branching in polyacrylates via midchain radical patching: a quantitative melt-state NMR study. *Macromolecules* **2010**, *43*, 5492−5495.
(52) Joseph Schork, F.; Luo, Y.; Smulders, W.; Russum, J. P.; Butté, A.; Fontenot, K. Miniemulsion Polymerization. *Polymer Particles*; Advances in Polymer Science; Springer, 2005; Vol. *175*, pp 129−255.
(53) Liu, X.; Lu, Y.; Luo, G. Continuous Flow Synthesis of Polystyrene Nanoparticles via Emulsion Polymerization Stabilized by a Mixed Nonionic and Anionic Emulsifier. *Ind. Eng. Chem. Res.* **2017**, *56*, 9489−9495.
(54) Daniloska, V.; Tomovska, R.; Asua, J. M. Designing tubular reactors to avoid clogging in high solids miniemulsion photopolymerization. *Chem. Eng. J.* **2013**, *222*, 136−141.

DOI: 10.1021/acs.iecr.9b03906
Ind. Eng. Chem. Res. 2019, 58, 21312−21322